

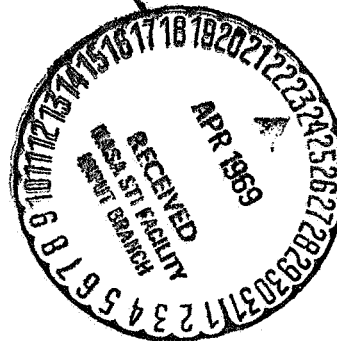
AED R-3426
February 15, 1969

Third Quarterly Report Action Of Lithium Radiation-Hardened Silicon Solar Cells

CASE FILE
COPY

Prepared for:
Jet Propulsion Laboratory
California Institute of Technology
Pasadena, California
In Fulfillment of:
Contract No. 952249

RCA



RCA Defense Electronic Products
Astro Electronics Division | Princeton, New Jersey

Third Quarterly Report: Action Of Lithium In Radiation-Hardened Silicon Solar Cells

Prepared for:
Jet Propulsion Laboratory
California Institute of Technology
Pasadena, California
In Fulfillment of:
Contract No. 952249
By
G. J. Brucker, T. J. Faith,
and A. G. Holmes-Siedle

RCA Defense Electronic Products
Astro Electronics Division | Princeton, New Jersey

NOTICE

This report contains information prepared by the Astro-Electronics Division of RCA under JPL subcontract. Its content is not necessarily endorsed by the Jet Propulsion Laboratory, California Institute of Technology, or the National Aeronautics and Space Administration.

PREFACE

This is the Third Quarterly Report on a program to study the "Action of Lithium in Radiation-Hardened Silicon Solar Cells." This report was prepared under Contract No. 952249 for Jet Propulsion Laboratory, Pasadena, California by the Astro-Electronics Division of RCA, Princeton, New Jersey. The period of performance covered by this report is from October 16, 1968 to January 15, 1969. The work reported here was conducted by the Advanced Techniques Group of the Astro-Electronics Division, Manager, Martin Wolf. The Physical Research Laboratory is located at the RCA Space Center. The Project Supervisor was Dr. A.G. Holmes-Siedle and the Project Scientist was Dr. G.J. Brucker. The Technical Monitor of the program was Mr. Paul Berman of JPL.

ABSTRACT

This is the Third Quarterly Report on a program of study and analysis of the manner in which lithium produces a recovery of radiation damage in silicon solar cells. This program has technical continuity with the work performed for NASA on Contract No. NAS5-10239. The eventual goal of this effort is to understand the recovery mechanism so that realistic predictions of solar-cell performance can be developed and optimum designs of lithium cells for space use can be specified.

The test vehicles being used for this work were (1) small-area solar-cell model devices, (2) a group of solar cells supplied by NASA on the above contract, (3) solar cells supplied by JPL, and (4) silicon bars, usually in the "Hall-bar" configuration. The source of particle irradiation used was a 1-MeV electron beam produced by the RCA Laboratories Van de Graaff generator.

The work during the present reporting period consisted of measurement of the physical properties and photovoltaic performance of a large number of JPL-furnished cells before irradiation and after recent irradiation to fluences of 1×10^{14} , 5×10^{14} , or 3×10^{15} e/cm². A total of thirty-two crucible-grown cells, irradiated to 1×10^{14} e/cm², have suffered no redegradation in a period extending to 69 days after irradiation. All except five cells (lot C2) have shown significant recovery, one group of five having higher power than n/p control cells irradiated to the same level. Float-Zone, Quartz-Crucible, and Lopex cells irradiated more recently have shown no redegradation in short-circuit current over a period extending to 11 days after irradiation. Some cells irradiated to 3×10^{15} e/cm², however, have developed shunt leakages during irradiation or have suffered increases in series resistance after irradiation. Measurements on five batches of Float-Zone cells (lot C4) with different lithium diffusion and redistribution schedules indicate a decrease in lithium density and increases in minority-carrier diffusion length and photovoltaic response with increasing redistribution time.

TABLE OF CONTENTS

Section	Page
I INTRODUCTION	1
A. General	1
B. Technical Approach	1
C. Summary of Preceding Work (Late 1967 to October 1968)	2
II PERFORMANCE OF JPL-FURNISHED CELLS	5
A. Introduction	5
B. C1, H1, and D-Cells	6
C. C2, H2, and T2 Cells	11
D. T3 and H4 Cells	16
E. C4 Cells	18
III CONCLUSIONS AND FUTURE PLANS	27
A. Conclusions	27
B. Future Plans	28
LIST OF REFERENCES	29

LIST OF ILLUSTRATIONS

Figure		Page
1	Cell Performance Vs. Time After Irradiation - C1(1) Cells	10
2	Cell Performance Vs. Time After Irradiation - H1(1) Cells	10
3	Cell Performance Vs. Time After Irradiation - C2(1) Cells	13
4	Cell Performance Vs. Time After Irradiation - H2(1) Cells	14
5	Cell Performance Vs. Time After Irradiation - T2(1) Cells	15
6	Cell Performance Vs. Time After Irradiation - T3(3) Cells	18
7	Cell Performance Vs. Time After Irradiation - C4(3) Cells	22
8	Cell Performance Vs. Time After Irradiation - C4(7) Cells	22
9	Cell Performance Vs. Time After Irradiation - C4(11) Cells	23
10	Cell Performance Vs. Time After Irradiation - C4(15) Cells	24
11	Cell Performance Vs. Time After Irradiation - C4(19) Cells	24
12	Pre-irradiation I-V Curves for Cell C4-32 at Two Light Levels . . .	25
13	Post-irradiation I-V Curves for Cell C4-32 Taken With 140 mw/cm ² Tungsten Illumination	25

LIST OF TABLES

Table		Page
I	Properties of C1 and H1 Cells	7
II	Photovoltaic Performance of C1 and H1 Cells	7
III	Photovoltaic Performance of n/p Control Cells	8
IV	Properties of C2, H2, and T2 Cells	12
V	Photovoltaic Performance of C2, H2, and T2 Cells	12
VI	Properties of T3 and H4 Cells	16
VII	Photovoltaic Performance of T3 and H4 Cells	17
VIII	Properties of C4 Cells	19
IX	Photovoltaic Performance of C4 Cells	20

SECTION I

INTRODUCTION

A. GENERAL

It has been shown that, at room temperature, electron, proton, and neutron-irradiated silicon solar cells spontaneously recover their electrical outputs following irradiation (Reference 1). Initially, the loss of electrical output is due to degradation of minority-carrier lifetime. The mobile lithium ion moves toward and combines with a defect-impurity complex, thereby changing its electrical properties. In solar cells, the interaction of lithium with radiation-induced defects ultimately produces a defect complex which appears to have little or no effect on the minority-carrier lifetime, the result being a near complete restoration of cell efficiency.

The contract effort reported here represents an experimental investigation of this phenomenon, by means of examining several of the physical properties of lithium-containing silicon bars and of p-on-n silicon solar-cells and by study of the processes that occur in these devices after irradiation. The objectives of the effort are to identify the parameters which effect the recovery and long-term stability characteristics of the solar cell structure and to generate information which will lead to the optimization of these parameters. The eventual goal is to exploit this phenomenon for the production of solar cells for the space environment in quantity. In this direction, it is anticipated that (1) realistic predictions of lithium-cell performance can ultimately be developed, and (2) optimum designs of lithium cells for space use can then be specified.

B. TECHNICAL APPROACH

Stated briefly, the approach to the objectives stated above involves the testing of bulk samples of silicon, fabricated in-house as well as government-furnished (GFE)¹

¹Government Furnished Equipment under Contract No. NAS5-10239.

cells and JPL-furnished² solar cells and in-house fabricated test diodes³. Experiments on bulk samples include Hall and resistivity measurements taken as functions of (1) 1-MeV electron fluence, (2) sample temperatures during irradiation, and (3) isochronal anneals.

C. SUMMARY OF PRECEDING WORK (Late 1967 to October 1968)

For purposes of continuity, a brief history is given here of the recent work performed on the predecessor contract (Reference 2) and the first half of the present contract. This history will also provide the reader with a better understanding of the current technical approach, its problems, and its objectives.

In the work of the past year under contract NAS5-10239, in addition to continuing a series of long-term stability tests on GFE¹ cells and initiating such tests on in-house fabricated test-diodes³ and a second group of GFE¹ cells, extensive measurements of cell capacitance were made over a wide range of reverse biases on selected solar cells and test diodes. These measurements yielded useful data on the variation of lithium donor-density vs. distance from the junction, and revealed large lithium-density gradients ($\sim 10^{19}\text{cm}^{-4}$) near the junction and extending more than $10\text{ }\mu\text{m}$ from the junction. The capacitance measurement also produced the observation that lithium motion could be detected in a solar cell under strong reverse bias and an effective lithium diffusion constant for the cell material could be established. The large lithium gradient also sets up a large internal electric field ($>100\text{ V/cm}$ near the junction edge) thereby creating a field-aided diffusion situation for minority-carriers. This effect invalidates the concept of diffusion length for small minority-carrier lifetimes, (i. e. , where the electric-field effect is significant over a large fraction of the current-collection volume). This is the case after irradiation to fluences of the order 10^{15} to 10^{16} MeV/cm^2 , making application of Waite's theory (Reference 3) very difficult. Accordingly, in the past year, some kinetic studies of damage recovery were made at lower radiation levels, in the fluence range 10^{13} to 10^{14} e/cm^2 . Waite's theory, which reduces to a first-order kinetic equation at these fluences, was shown to describe the experimental recovery curves adequately for a large number of cells. These cells, cells irradiated to $\sim 10^{15}\text{ e/cm}^2$, and unirradiated cells, have since been

²Lithium-diffused cells delivered by JPL to RCA for evaluation as part of this contract effort.

³Test vehicles, similar to solar cells in all but photovoltaic response, fabricated so as to be compatible with experiments which appear particularly promising in terms of information yield, as well as the experiments which are regularly performed in the course of the work. These test vehicles include both lithium-diffused and non-lithium-diffused diodes.

undergoing long-term monitoring of their characteristics for stability of (1) minority-carrier diffusion length, and (2) photovoltaic I-V characteristics.

The problem of redegradation of recovered cells was attacked. Long-term stability tests made during the preceding contract and the first half of the present contract (Reference 4) on lithium-doped cells irradiated to fluences from 10^{14} to 10^{16} e/cm² indicated that devices made from low-oxygen-content (Lopex or Float-Zone) silicon are more likely to remain stable after recovery for radiation damage if the lithium-density concentration is sufficiently low to avoid significant lithium movement in the region near the junction. Several lithium cells which redegraded after irradiation to 10^{14} e/cm², and one which degraded spontaneously with no irradiation, displayed post-degradation photovoltaic characteristics which were not explainable in terms of straightforward solar-cell equivalent circuits. In most redegrading cells, the short-circuit current showed no sensible redegradation during power and open-circuit voltage redegradation. Minority-carrier diffusion length was also relatively constant during redegradation.

In the first half of the present contract, silicon Hall bars of two types of crystal growth and two lithium concentrations were bombarded at about twenty controlled temperature (T_B) levels between liquid - nitrogen (79°K) and 280°K. At all temperatures, carrier-removal rates ($\Delta n / \Delta \Phi$) were found to be lower than for Stein's (Reference 5) comparable irradiations of phosphorus-doped silicon. The difference was greatest at the low temperatures. Introduction rates of carrier-removal defects were exponentially dependent on the reciprocal of bombardment temperature for both types of crystal growth, but the slopes and limiting temperature values differed. The temperature dependence was not consistent with a simple charge-state-dependent probability of interstitial-vacancy dissociation and impurity-vacancy trapping.

Following bombardment, the temperature dependence of the carrier concentration and carrier mobility in the lithium-doped samples was measured periodically in the conventional manner. A characteristic pattern of reappearance of carriers (annealing of carrier removal) and disappearance of charged-scattering centers (annealing of mobility) was observed in Float-Zone refined silicon at room temperature. Such recoveries did not occur so strongly in crucible-grown silicon and a different pattern of recovery was observed in this oxygen-rich material. It was previously thought that, while lithium would be removed during the formation of the second complex or "recovered-damage center", no net change in carrier concentration would occur. The partial annealing of carrier removal in Float-Zone silicon indicated an unexpected partial dissociation of the first complex (Li-V) which, however, does not occur when oxygen is present.

The above Hall-measurement results suggest that a lithium-oxygen-vacancy (Li-O-V) complex is produced by electron bombardment in Quartz-Crucible silicon, and a lithium-vacancy (Li-V) complex in zone-refined silicon. The mechanism of

room-temperature annealing is attributed to neutralization of carrier-removal defects by lithium interaction in crucible silicon, and by both lithium interaction and defect dissociation in zone silicon. The Li-V defect is loosely bound compared to the oxygen containing Li-O-V defect.

SECTION II

PERFORMANCE OF JPL-FURNISHED CELLS

A. INTRODUCTION

During the present reporting period, effort was concentrated on the evaluation of lithium-diffused p/n solar cells supplied by JPL. To date, three shipments have been received. The first shipment contained ten crucible-grown cells (termed "C1 cells") with 100 to 200 ohm-cm starting resistivity and ten crucible-grown cells ("H1-cells") with 25 to 35 ohm-cm starting resistivity. Shipment No. 2 contained ten crucible-grown cells ("C2-cells") with 5 to 10 ohm-cm starting resistivity, ten crucible-grown cells ("H2-cells") with 20 ohm-cm starting resistivity, and ten crucible-grown cells ("T2-cells") with starting resistivity greater than 20 ohm-cm. Shipment No. 3 contained fifteen Lopex⁴ cells ("T3-cells") with starting resistivity greater than 50 ohm-cm, ten Float-Zone cells ("H4-cells") with 80 to 120 ohm-cm starting resistivity, sixty Float-Zone cells ("C4-cells") with 200 ohm-cm starting resistivity, and fifty 10 ohm-cm n/p cells ("D-cells").

Tests performed on the cells included measurements of photovoltaic response under unfiltered tungsten illumination and air-mass-zero short-circuit current, extrapolated from filter wheel measurements (Reference 6), measurements of p/n junction characteristics in the dark, reverse-bias capacitance measurements to obtain donor-density profiles, and minority-carrier diffusion length measurements. The tungsten I-V characteristics have been measured with a power density of 140 mW/cm² incident on the cell surface. The cell temperature is maintained at 28°C by water and forced-air cooling. The measurements are reproducible over several years to within approximately 2 percent. In addition to the measurements at 140 mW/cm², comparative I-V characteristics were frequently taken at a number of light levels. Measurements of this sort provide information on cell series resistance and junction characteristics (Reference 7).

⁴Trademark of Texas Instruments, Inc.

Such measured cells were irradiated by 1-MeV electrons to one of three fluence values⁵: 1×10^{14} , 5×10^{14} or 3×10^{15} e/cm². All irradiations were made at a rate of approximately 3×10^{13} e/cm²/min. Several cells, however, were not irradiated, in order to provide a test of whether or not redegradation is induced by radiation.

Measurements after irradiation have consisted mainly of taking I-V characteristics under 140 mW/cm² tungsten light. Measurements were repeated periodically, to determine the recovery and stability properties of the test cells. Wherever appropriate, such as when some cell redegradation was observed, multilevel tungsten I-V measurements, and capacitance and dark I-V measurements were made in order to determine the relationship between changes in I-V characteristics and the cell's physical properties.

In the material to follow, the cells will be discussed in separate paragraphs according to lot, i. e., lots C1, H1, and D(n/p control cells) in paragraph B, lots C2, H2, and T2 in paragraph C, lots T3 and H4 in paragraph D, and lot C4 in paragraph E. Cells from each lot are separated into several groups according to the fluence to which they have been exposed. These groups are indicated by the numbers in parentheses, e. g., lot C2 is in three groups; C2(1) exposed to 1×10^{14} e/cm²; C2(2) exposed to 5×10^{14} e/cm²; and C2(3) exposed to 3×10^{15} e/cm². In discussing cell performance, the average for a given group will be presented. Individual cells will be discussed only when their behavior diverges significantly from that of the group to which they belong.

B. C1, H1, AND D-CELLS

The C1 and H1 cells were made from Quartz-Crucible silicon as were the n/p D cells. The lithium diffusion and redistribution temperatures and times, the averaged initial lithium concentrations, and the diffusion lengths for C1 and H1 cells are given in Table I. Both C1 and H1 cells were divided into two groups. Groups C1(1) and H1(1), each consisting of 8 cells, were irradiated to a fluence of 1×10^{14} e/cm² in November 1968; groups C1(2) and H1(2), each consisting of 2 cells, were irradiated to a fluence of $\approx 8 \times 10^{14}$ e/cm² of ≈ 0.7 MeV electrons in January 1969.

In Table I, N_{LO} is the lithium density (cm⁻³) at the edge of the depletion region, i. e., approximately 1 μ m from the junction, and dN_L/dw is the lithium density gradient (cm⁻⁴) giving the increase in lithium density with distance from the depletion edge.

⁵In one of the irradiations, due to an error, cells were exposed to $\approx 8 \times 10^{14}$ e/cm² of ≈ 0.7 MeV electrons instead of the intended 5×10^{14} e/cm² of 1-MeV electrons.

N_{LO} is calculated from capacitance measurements taken near zero-bias, and dN_L/dw is obtained from capacitance measurements with the cell at reverse bias. Past measurements on lithium cells (Reference 2) have shown an approximately linear increase in lithium density with distance from the edge of the depletion region, i. e., constant dN_L/dw , for a region extending several microns beyond the depletion edge. This was also found to be the case in the C1 and H1 cells (Reference 4b.) It is seen from Table I that the shorter lithium diffusion time in C1 cells (5 minutes as compared to 90 minutes in H1 cells), has resulted in a very low lithium density, N_{LO} , and density gradient, dN_L/dw . The C1 cells also have a high pre-bombardment diffusion length, $L_0 = 115 \mu m$, whereas the H1 cells have a much lower value, $L_0 = 29 \mu m$.

TABLE I
PROPERTIES OF C1 AND H1 CELLS

Cell Group	Number of Cells	(e/cm^2) ϕ	Li diffusion		Li redistribution		Li concentration		(μm) L_0
			Temp($^{\circ}C$)	Time(Min)	Temp($^{\circ}C$)	Time(Min)	$N_{LO}(cm^{-3})$	$dN_L/dw(cm^{-4})$	
C1(1)	8	1×10^{14}	450	5	450	40	$< 10^{14}$	1×10^{18}	110
C1(2)	2	$\approx 8 \times 10^{14}^*$	450	5	450	40	$< 10^{14}$	1×10^{18}	130
H1(1)	8	1×10^{14}	425	90	425	60	5×10^{14}	2×10^{19}	30
H1(2)	2	$\approx 8 \times 10^{14}^*$	425	90	425	60	5×10^{14}	2×10^{19}	20

* ≈ 0.7 MeV electrons

Table II gives the photovoltaic response curves of the cells, under illumination by 140 mW/cm^2 of tungsten light, measured before irradiation and several times after irradiation. The values are averaged over all the cells of the group (except when otherwise specified), with I_0 being the pre-irradiation short-circuit current, P_0 as the power at the maximum power point, and V_0 as the open-circuit voltage. For convenience, the post-irradiation values I , P , and V are normalized to the initial values. The first set of measurements after irradiation is listed as "post-irradiation" in Table II (and in tables to follow) and was taken within 30 minutes after irradiation. All subsequent sets of measurements are labelled with the number of days (or minutes) elapsed after irradiation.

TABLE II
PHOTOVOLTAIC PERFORMANCE OF C1 AND H1 CELLS

Cell Group	(e/cm^2) ϕ	Pre-irradiation			Post-irradiation			7 Days*			45 Days			69 Days		
		$I_0(mA)$	$P_0(mW)$	$V_0(mV)$	I/I_0	P/P_0	V/V_0	I/I_0	P/P_0	V/V_0	I/I_0	P/P_0	V/V_0	I/I_0	P/P_0	V/V_0
C1(1)	1×10^{14}	71.0	30.3	600	0.69	0.61	0.86	0.70	0.61	0.86	0.71	0.64	0.87	0.73	0.65	0.87
C1(2)	5×10^{14}	72.0	31.8	605	0.54	0.43	0.80	0.55	0.44	0.79						
H1(1)	1×10^{14}	57.0	21.7	565	0.73	0.72	0.93	0.79	0.79	0.94				0.91	0.94	0.97
H1(2)	5×10^{14}	45.2	17.4	544	0.68	0.62	0.90	0.72	0.66	0.89						

*11 days for Groups C1(2) and H1(2)

Table III gives similar pre-irradiation and post-irradiation values for 10 ohm-cm n/p cells. This table gives values for cells irradiated to 5×10^{14} and $3 \times 10^{15} \text{e/cm}^2$ of 1 MeV electrons, in addition to those for cells irradiated to $1 \times 10^{14} \text{e/cm}^2$ of 1 MeV electrons and $\approx 8 \times 10^{14} \text{e/cm}^2$ of ≈ 0.7 MeV electrons, and will be referred to as a basis of comparison for all lithium cells in the present report. In comparing Tables II and III, it is noteworthy that the C1 cells have higher initial photovoltaic parameters than the n/p cells. The values averaged over all ten C1 cells were: $I_o = 71.2 \text{ mA}$, $P_o = 30.6 \text{ mW}$, and $V_o = 600 \text{ mV}$; those averaged over the fourteen n/p cells were: $I_o = 69.5 \text{ mA}$, $P_o = 28.1 \text{ mW}$, and $V_o = 553 \text{ mV}$. Thus both the power and the short-circuit current in the C1 cells was higher than in the n/p cells. This was true in spite of the fact that the averaged diffusion length in the n/p cells, $L_o = 170 \mu\text{m}$, was significantly higher than the $115 \mu\text{m}$ average for the C1 cells. This observation is in agreement with previous observations (Reference 8) which indicated that, for a given diffusion length, lithium cells yield a higher short-circuit current than n/p cells. The higher open-circuit voltages in the lithium cells is not fully understood (note the relatively low lithium density in the C1 cells) but observations of V_o increase during lithium diffusion have been reported by the manufacturer (Reference 9).

TABLE III
PHOTOVOLTAIC PERFORMANCE OF n/p CONTROL CELLS

Control Cell	ϕ (e/cm^2)	Pre-irradiation			Post-irradiation		
		$I_o(\text{mA})$	$P_o(\text{mW})$	$V_o(\text{mV})$	I/I_o	P/P_o	V/V_o
D-1	1×10^{14}	68.9	28.2	553	0.81	0.75	0.93
D-2	1×10^{14}	69.5	28.0	555	0.81	0.76	0.94
D-3	1×10^{14}	71.0	28.4	552	0.82	0.77	0.93
D-4	1×10^{14}	69.1	27.7	553	0.83	0.77	0.93
D-5	5×10^{14}	69.0	28.1	557	0.71	0.63	0.90
D-6	5×10^{14}	73.0	28.2	555	0.69	0.62	0.90
D-7	$\approx 8 \times 10^{14}*$	69.3	28.6	557	0.69	0.59	0.87
D-8	$\approx 8 \times 10^{14}*$	71.0	28.1	550	0.66	0.58	0.88
D-9	3×10^{15}	67.3	27.9	551	0.59	0.49	0.85
D-10	3×10^{15}	69.0	28.6	551	0.59	0.49	0.85
D-11	3×10^{15}	68.1	27.7	550	0.59	0.50	0.86
D-12	3×10^{15}	72.0	29.3	555	0.57	0.47	0.85
D-13	5×10^{14}	69.2	27.3	548	0.72	0.66	0.91
D-14	5×10^{14}	67.2	27.4	554	0.72	0.64	0.90

* ≈ 0.7 MeV electrons

The H1 cells have significantly lower pre-irradiation values than the n/p cells, the averages being $I_o = 52.6 \text{ mA}$, $P_o = 20.7 \text{ mW}$, and $V_o = 561 \text{ mV}$. The lower values of short-circuit current are partly due to the lower minority-carrier lifetime in the

H1 cells ($L_0 = 29 \mu\text{m}$). However, they are also due in part to the nature of the spectrum of the tungsten light used in the tests. The tungsten source has higher relative intensity toward the red end of the spectrum than does light from the sun which is further shifted to the blue. Since red light has a lower absorption coefficient in silicon than blue light, minority carriers are generated (on the average) deeper in the base region with tungsten light than with sunlight. Thus, cell performance is much more sensitive to diffusion length under tungsten illumination than under sunlight, and the H1 cells will perform better under sunlight than the numbers in Table II indicate. An attempt was made to overcome this shortcoming by calculating air-mass-zero short-circuit current of the cells applying a standard technique (Reference 6) which utilizes measurements of short-circuit current under light from a three-color filter-wheel system. Later, these filter wheel measurements were compared with I-V curves made on lot C4 cells with a solar simulator (Reference 10). The comparison showed the filter wheel value of I_0 to be ~ 10 percent below the simulator value. A probable explanation of this discrepancy lies in the previous observation, by Brucker, et al (Reference 8), of a strong injection-level (or light level) dependence of the diffusion length in lithium-containing solar cells. Given the comparison with the simulator, and the fact that the light level in each filter wheel measurement is more than a factor of 10 below the sunlight level at air-mass-zero, the filter-wheel measurements were concluded to be misleading and were discontinued.

As stated previously, post-irradiation values under tungsten illumination, normalized to the corresponding pre-irradiation values, are given in Tables II and III. The post-irradiation elapsed time for groups C1(2) and H1(2) is not sufficient yet to cite any trends. However, trends for groups C1(1) and H1(1) emerge clearly in Figures 1 and 2. These figures present the averaged values of Table II plotted against time after bombardment in days. A scale also indicates the absolute value of the average of the maximum power of these groups of cells. In order to compare the cells performance to n/p cells, the post-irradiation power values for D-1 and D-2 (two typical n/p cells irradiated to $1 \times 10^{14} \text{e/cm}^2$) are indicated on each scale.

The C1(1) cells, shown in Figure 1, display a very slow rate of recovery over the first 69 days after irradiation. Over this time, the average power recovered from 18.6 mW ($0.61 P_0$) to 19.8 mW ($0.65 P_0$). If this rate of recovery were maintained, approximately three more months would pass before the average reached the 21.4 mW of the n/p control cells. This very slow recovery is not surprising, in view of the very low lithium density in these cells. Only one of the cells in group C1(1) has shown any tendency to degrade. This was cell C1-30 which continued to decrease in performance for a period of several days after irradiation had ceased. Immediately after irradiation, the performance values were $I = 49.5 \text{ mA}$, $P = 18.0 \text{ mW}$, and $V = 515 \text{ mV}$. Seven days after bombardment, they had decreased to $I = 46.9 \text{ mA}$, $P = 16.6 \text{ mW}$, and $V = 500 \text{ mV}$. Subsequent readings, however, showed a steady increase: 69 days after irradiation, $I = 48.2 \text{ mA}$, $P = 17.4 \text{ mW}$, and $V = 507 \text{ mV}$. The values for this cell are still several percent below the group average.

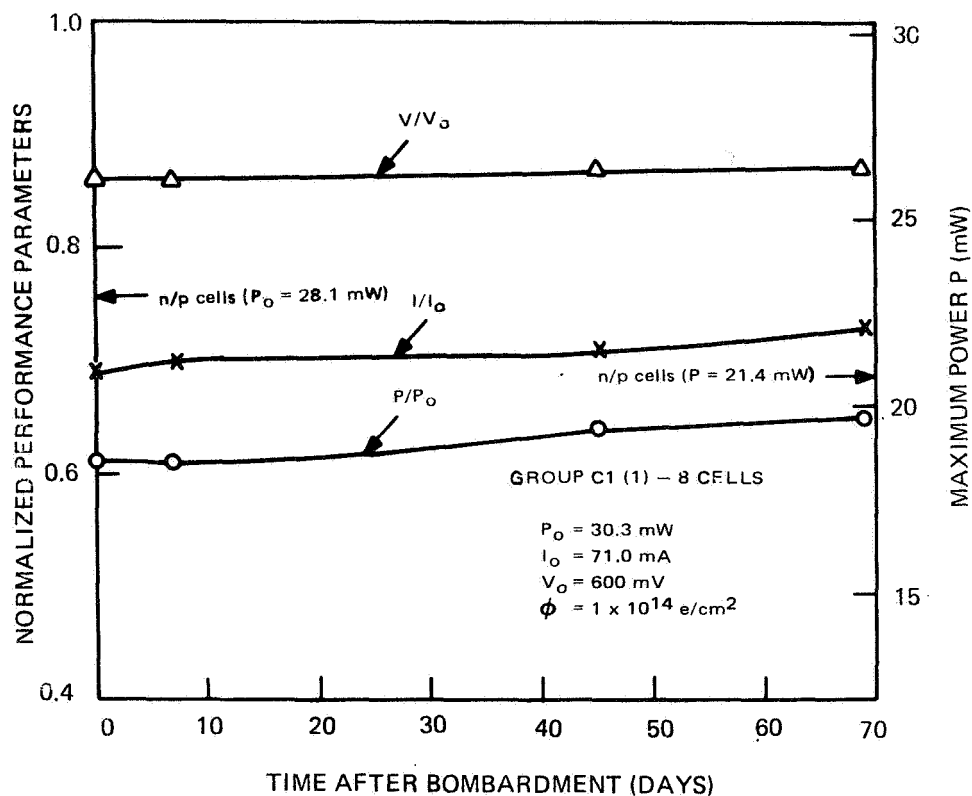


Figure 1. Cell Performance vs. Time After Irradiation to $1 \times 10^{14} \text{ e/cm}^2$ - C1(1) Cells

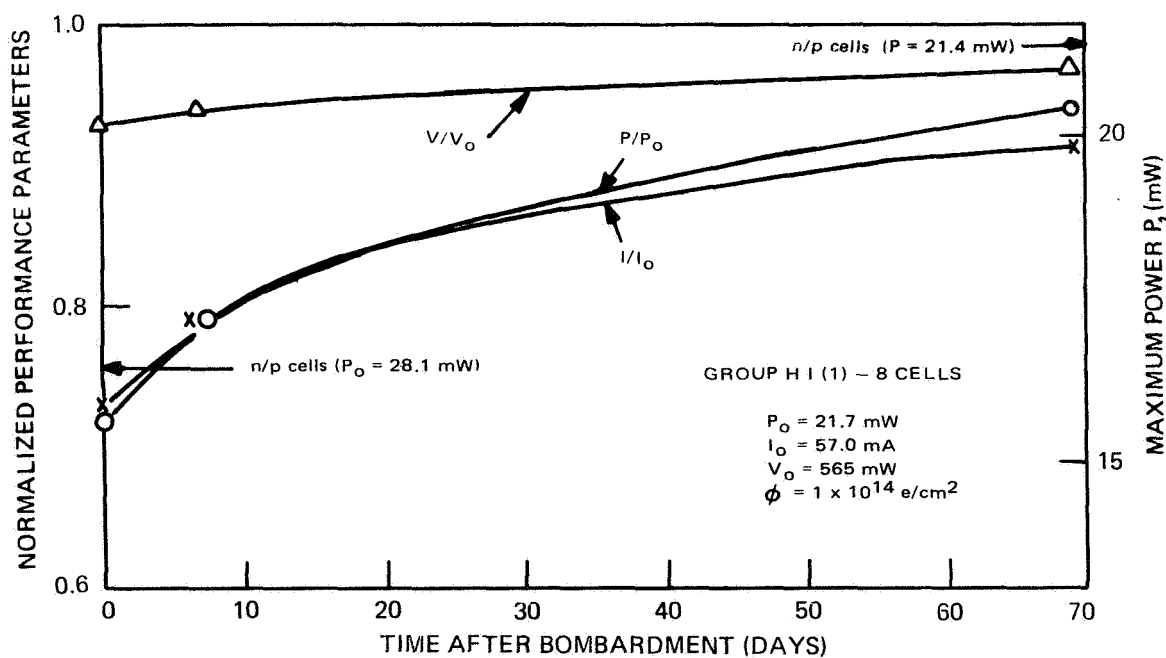


Figure 2. Cell Performance vs. Time After Irradiation to $1 \times 10^{14} \text{ e/cm}^2$ - H1(1) Cells

The cells of group H1(1) recovered much more rapidly as can be seen in Figure 2. From immediately after irradiation to 69 days after irradiation, the averaged power recovered from 15.7 mW (0.72 P_O) to 20.3 mW (0.94 P_O) so that the averaged power of the H1(1) cells is now higher than that of the C1(1) cells. Note that the percentage power loss during bombardment is also lower in H1(1) cells (28 percent) than in C1(1) cells (39 percent). This is a consequence of the lower initial power in the H1(1) cells. In order to achieve the same power level as n/p cells irradiated to $10^{14}e/cm^2$, the H1(1) cells will have to recover to $\approx 0.99 P_O$. The post-irradiation behavior has been similar for all of the H1(1) cells, and there were no instances of redegradation. However, the spread in initial performance was rather large and, thus, worth noting. The highest value of I_O was 57.1 mA; the lowest, 50.5 mA. The highest value of P_O was 23.2 mW; the lowest, 19.2 mW.

C. C2, H2, AND T2 CELLS

All of the cells in lot 2 were made from Quartz-Crucible silicon. The lithium diffusion and redistribution temperatures and times, as well as the averaged initial lithium concentrations⁶ and minority-carrier diffusion lengths, are given in Table IV. The C2, H2, and T2 cells are each divided into three groups: (1) cells exposed to $1 \times 10^{14}e/cm^2$, (2) cells exposed to $5 \times 10^{14}e/cm^2$, and (3) cells exposed to $3 \times 10^{15}e/cm^2$.

The lithium density in the C2 cells, as determined by capacitance measurements vs. reverse bias, varied a good deal from cell to cell. The cells of lot H2 had densities similar to those of H1 cells, while T2 cells had lower densities, similar to those of C1 cells. The average pre-bombardment diffusion lengths were: C2 cells $\approx 80 \mu m$; H2 cells $\approx 40 \mu m$; and T2 cells $\approx 90 \mu m$.

Table V gives pre- and post-irradiation performance parameters for each group. Note that group (1) cells from each manufacturer have been separated from the corresponding groups (2) and (3) in the table since the $1 \times 10^{14}e/cm^2$ exposure was carried out in November 1968, while the 5×10^{14} and $3 \times 10^{15}e/cm^2$ exposures were done in January 1969.

⁶In these and subsequent data, concentrations given are only approximate, being calculated from the data of one cell from a group. However, a computer program is presently being put into operation to compute all lithium densities from the raw capacitance data and these more accurate results should be available shortly.

TABLE IV
PROPERTIES OF C2, H2, AND T2 CELLS

Cell Group	Number of Cells	(e/cm ²) ϕ	Li Diffusion		Li Redistribution		Li Concentration		(μm) L_o
			Temp(°C)	Time(Min)	Temp(°C)	Time(Min)	$N_{LO}(\text{cm}^{-3})$	$dN_L/dw(\text{cm}^{-4})$	
C2(1)	5	1×10^{14}	425	90	425	120	wide range		80
C2(2)	2	5×10^{14}	425	90	425	120	wide range		80
C2(3)	3	3×10^{15}	425	90	425	120	wide range		80
H2(1)	5	1×10^{14}	425	90	425	60	5×10^{14}	1×10^{19}	40
H2(2)	2	5×10^{14}	425	90	425	60	5×10^{14}	1×10^{19}	40
H2(3)	3	3×10^{15}	425	90	425	60	5×10^{14}	1×10^{19}	40
T2(1)	6	1×10^{14}	400	90	400	120	2×10^{14}	1×10^{18}	90
T2(2)	2	5×10^{14}	400	90	400	120	2×10^{14}	1×10^{18}	90
T2(3)	2	3×10^{15}	400	90	400	120	2×10^{14}	1×10^{18}	90

TABLE V
PHOTOVOLTAIC PERFORMANCE OF C2, H2, AND T2 CELLS

Cell Group	(e/cm ²) ϕ	Pre-irradiation			Post-irradiation			45 Days			69 Days		
		$I_o(\text{mA})$	$P_o(\text{mW})$	$V_o(\text{mV})$	I/I_o	P/P_o	V/V_o	I/I_o	P/P_o	V/V_o	I/I_o	P/P_o	V/V_o
C2(1)	1×10^{14}	66.8	29.6	592	0.69	0.59	0.87	0.70	0.61	0.87	0.70	0.61	0.87
H2(1)	1×10^{14}	61.9	26.0	583	0.71	0.65	0.89	0.92	0.87	0.95	0.92	0.88	0.95
T2(1)	1×10^{14}	68.2	26.8	583	0.71	0.62	0.87	0.93	0.88	0.96	0.92	0.88	0.96
		Pre-irradiation			Post-irradiation			3 Days			11 Days		
C2(2)	5×10^{14}	68.0	30.3	592	0.59	0.49	0.83	0.59	0.50	0.83	0.61	0.50	0.83
C2(3)	3×10^{15}	67.6	30.1	593	0.45	0.36*	0.77*	-	-	-	0.47	0.37*	0.76*
H2(2)	5×10^{14}	57.3	24.3	578	0.65	0.56	0.86	0.65	0.56	0.86	0.68	0.57	0.86
H2(3)	3×10^{15}	59.7	25.2	582	0.49	0.39	0.79	0.49	0.39	0.79	0.50	0.39	0.78
**T2(2)	5×10^{14}	69.3	26.4	577	0.53	0.48	0.83	0.79	0.67	0.87	0.87	0.76	0.90
***T2(3)	3×10^{15}	68.8	25.3	576	0.46	0.33	0.73	0.50	0.30	0.71	0.56	0.33	0.72

*One cell (with shunt leakage) not included

**Readings for one cell only; other cell displays shunt leakage

***Both cells display severe post-bombardment shunt leakage and series resistance

Considering first cells of group (1), Figures 3, 4, and 5 graphically illustrate the data given in Table V for cell groups C2(1), H2(1), and T2(1), respectively. Cells of the C2(1) group displayed good initial characteristics ($P_o = 29.6$ mW). However, they have shown almost no recovery in the 69 days since exposure to radiation. The short-circuit current has increased only from $0.69 I_o$ to $0.71 I_o$ and the power from $0.59 P_o$ to $0.60 P_o$. All of the cells except one (C2-12, which displayed significant shunt leakage after bombardment) behave similarly after bombardment in spite of large cell-to-cell variations in measured donor density profile. The absence of significant recovery is puzzling. It is possible at this time only to conjecture that some impurity is completely bonding with and, thereby, immobilizing the lithium. The relatively low starting resistivity (i.e., low for lithium cells) of 5 to 10 ohm-cm and the antimony dopant are other possible factors. However, more information is required on these cells, especially with regard to the behavior of the donor density profile with respect to time, in order to draw any solid conclusions.

The cells of group H2(1) also had reasonably good initial performance ($P_o = 26.0$ mW). The recovery, shown in Figure 4, is from $0.65 P_o$ immediately after irradiation to $0.88 P_o$ sixty-nine days after irradiation, giving the H2(1) cells an averaged power of 22.9 mW, significantly above the average of two 10 ohm-cm n/p cells irradiated to the same fluence. None of the cells of this group showed any erratic behavior.

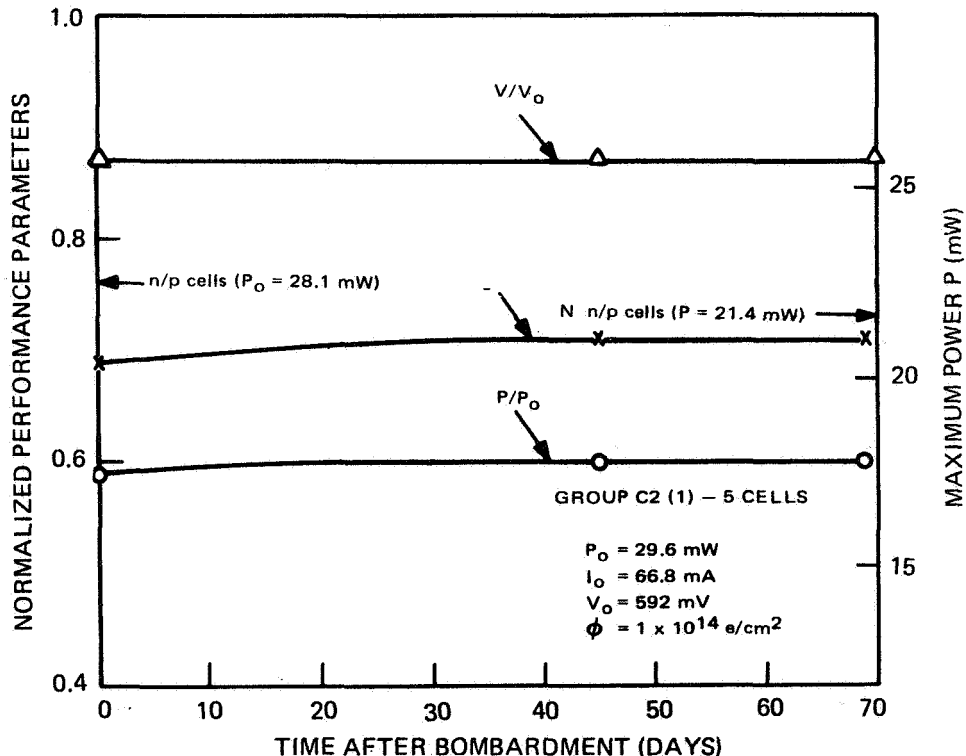


Figure 3. Cell Performance vs. Time After Irradiation to $1 \times 10^{14} \text{e/cm}^2$ - C2(1) Cells

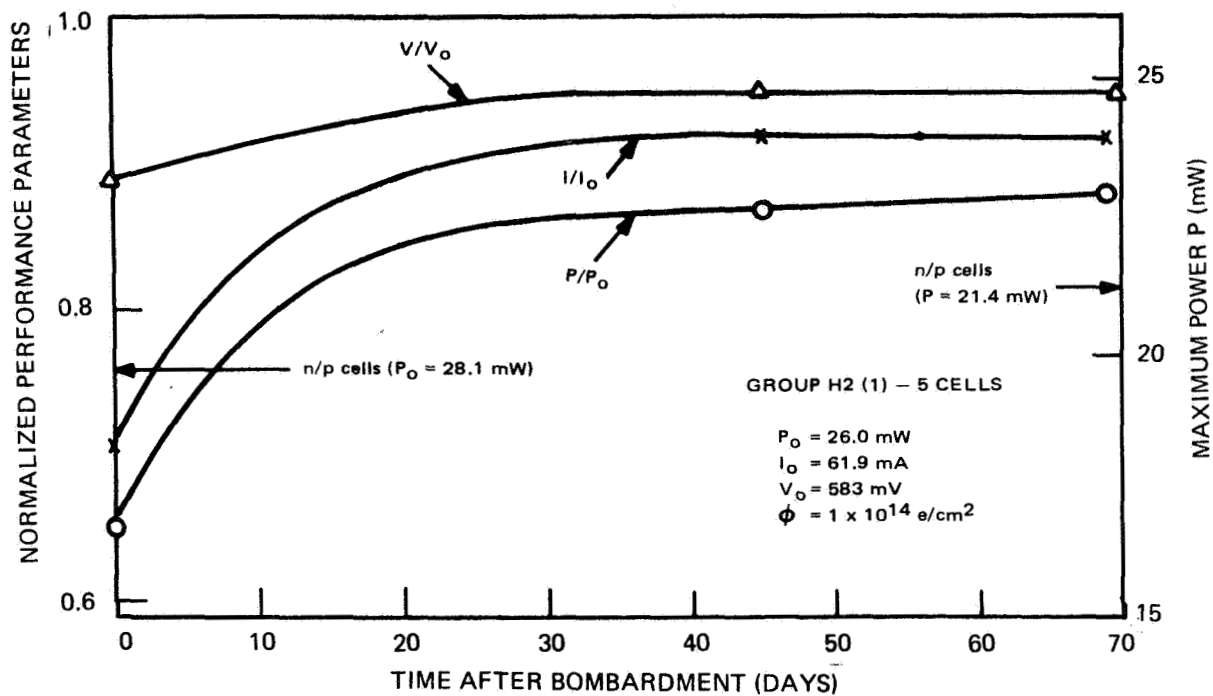


Figure 4. Cell Performance vs. Time After Irradiation to 1×10^{14} e/cm² - H2(1) Cells

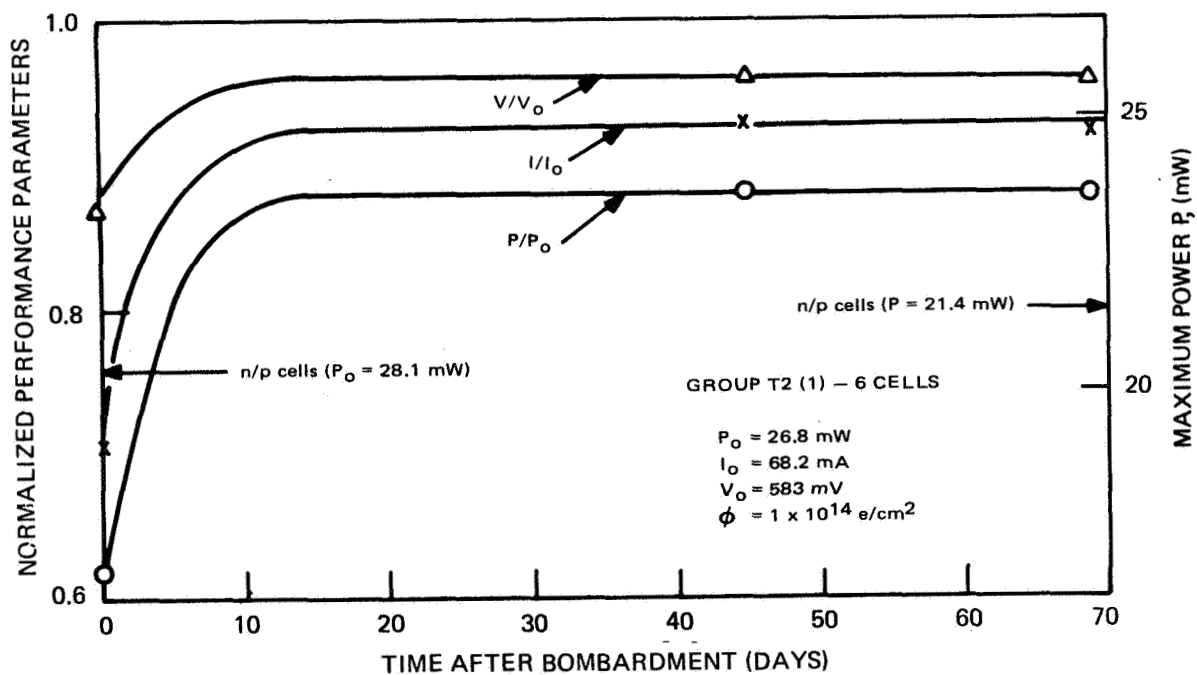


Figure 5. Cell Performance vs. Time After Irradiation to 1×10^{14} e/cm² - T2(1) Cells

The T2(1) cells had high short-circuit current, $I_0 = 68.2$, but the photovoltaic characteristics had a rather low curve power factor of 0.67. (The averaged power factors for groups C2(1) and H2(1) were 0.75 and 0.72, respectively.) Thus, the initial power for group T2(1) was only 26.8 mW. The A factor of the cells was obtained using multi-light-level I-V characteristics (Reference 7), and was found to be close to unity in the current range of interest, 30 to 65 mA. However, the cells were found to have approximately 1-ohm series resistance (as compared with ≈ 0.3 ohm for C2(1) and H2(1) cells). This series resistance was probably largely responsible for the low curve power factor in these T2(1) cells.

The post-irradiation behavior of the T2(1) cells is shown in Figure 5. These cells recovered surprisingly rapidly (within ≈ 10 days as indicated by spot checks on individual cells not indicated in Figure 5). The recovery was particularly rapid considering the low lithium density in the T2 cells and it is suspected that the oxygen density in these cells is considerably below that normally encountered in Quartz-Crucible cells. The cells have maintained substantially stable performance between the 45th and 69th day after irradiation. The post-irradiation series resistance is ≈ 1 ohm, the same as the pre-irradiation value. Only one instance of erratic behavior, a ≈ 200 ohm shunt leakage in T2-16 on the 45th day, has been observed. This shunt leakage was not present in the most recent readings.

Table V also gives post-irradiation values for lot 2 cells of groups (2) and (3). These tests extend only eleven days after irradiation, however, some interesting trends are already evident. First, one of the cells of group C2(3), cell C2-20 developed a shunt leakage of 100 ohms immediately after irradiation to $3 \times 10^{15} \text{e/cm}^2$ and was dropped from the average in Table V. The other two cells from this group, C2-19 and C2-21, also developed less severe shunt leakages of ≈ 300 ohms, apparently during irradiation. The shunt leakage in all of these cells has remained constant since irradiation. The series resistance of the cells is less than 1 ohm. In addition, severe shunt leakages appeared in both cells of group T2(3) after irradiation to $3 \times 10^{15} \text{e/cm}^2$. These leakages are reflected in the low post-irradiation values of P/P_0 in Table V. One of the cells, T2-19, has had a ≈ 100 ohm leakage since irradiation accompanied by a series resistance of ≈ 2 ohm immediately after irradiation which has subsequently increased with time. The other cell, T2-18, displayed a shunt resistance varying in time: > 200 ohms immediately after irradiation, ≈ 33 ohms at 3 days, and ≈ 100 ohms at 11 days. T2-18 also showed a series resistance increase from ≈ 1 ohm to ≈ 1.5 ohms during irradiation with no subsequent post-irradiation increase in series resistance. The reason for the shunt resistances is not clear. However, the increase in series resistance in the relatively lightly doped T2(3) cells after the heavy, $3 \times 10^{15} \text{e/cm}^2$, irradiation could be caused by carrier removal. Unfortunately, there is no readily available method to check this since the capacitance method for obtaining donor density is invalid when the defect density is comparable to the donor density (Reference 11).

It should be noted that one of the two T2(2) cells, T2-14, has a severe shunt leakage of ~ 50 ohms. However, this was present even before irradiation. The remaining cells in groups (2) and (3) of lot 2 display no irregular behavior up to the present time.

D. T3 AND H4 CELLS

Cells from lot T3 were manufactured from phosphorus doped Lopex silicon with starting resistivity of greater than 50 ohm-cm. Cells from lot H4 were made from phosphorus-doped Float-Zone silicon with starting resistivity of ≈ 100 ohm-cm. The process variables, approximate initial lithium concentrations, and initial diffusion lengths are listed in Table VI. T3 cells are seen to have very high lithium densities, $N_{LO} \sim 3 \times 10^{15} \text{ cm}^{-3}$, $dN_L/dw \sim 10^{20} \text{ cm}^{-4}$, but also high diffusion lengths $\approx 80 \mu\text{m}$. These cells, together with Texas Instruments Lopex and Float-Zone cells received under a predecessor NASA contract (Reference 2), prove that high lithium doping and high minority carrier lifetime are not necessarily incompatible. The cells from lot H4 also have high lithium density near the junction, a factor of ~ 3 below that for the T3 cells. The H4 cells, however, have low diffusion lengths, the average being approximately $30 \mu\text{m}$.

Considerable difficulty was encountered in the measurement of the properties of both T3 cells and H4 cells. The problem with T3 cells arose due to intermittent shunt leakages. Such shunt leakage was encountered during both dark and illuminated I-V measurements although, in general, it became more severe with increasing illumination. Spontaneous changes were frequently encountered during the course of a measurement. It is tentatively concluded that the cell leakage was internal. Given the high doping density of these cells, it is possible that precipitates could form in the junction region, giving rise to shunt leakage. In any case, the leakage rendered several cells, namely T3-17, -21, -27, -28, -29, and -30, useless for testing purposes, and several others, as will be seen below, questionable as to measurements of power and open-circuit voltage.

TABLE VI
PROPERTIES OF T3 AND H4 CELLS

Cell Group	Number of Cells	(e/cm^2) ϕ	Li Diffusion		Li Redistribution		Li Concentration		(μm) L_0
			Temp($^{\circ}\text{C}$)	Time(Min)	Temp($^{\circ}\text{C}$)	Time(Min)	$N_{LO}(\text{cm}^{-3})$	$dN_L/dw(\text{cm}^{-4})$	
T3(1)	3	1×10^{14}	400	90	0	0	3×10^{15}	1×10^{20}	80
T3(2)	3	$\approx 8 \times 10^{14}^*$	400	90	0	0	3×10^{15}	1×10^{20}	80
T3(3)	3	3×10^{15}	400	90	0	0	3×10^{15}	1×10^{20}	80
H4(1)	2	1×10^{14}	425	90	425	60	1×10^{15}	3×10^{19}	30
H4(2)	3	$\approx 8 \times 10^{14}^*$	425	90	425	60	1×10^{15}	3×10^{19}	30

*Electron energy: approx. 0.7 MeV

The H4 cells presented contact problems. On many of the cells it was not possible to obtain good contact. This problem was alleviated in the case of some cells by applying solder to one of the corner darts of the top contact. However, proper contact has not been obtained to cells H4-39⁷, -42, or -53.

The T3 cells were divided into three groups which were irradiated to $1 \times 10^{14} \text{e/cm}^2$, $\approx 8 \times 10^{14} \text{e/cm}^2$ of $\approx 0.7 \text{ MeV}$ electrons, and $3 \times 10^{15} \text{e/cm}^2$. The H4 cells were divided into 2 groups irradiated to $1 \times 10^{14} \text{e/cm}^2$ and $\approx 8 \times 10^{14} \text{e/cm}^2$ of $\approx 0.7 \text{ MeV}$ electrons. Table VII lists the results of the pre-irradiation and post-irradiation measurements on these five groups of cells. In groups T3(1) and T3(2) irradiated to $1 \times 10^{14} \text{e/cm}^2$ and $\approx 8 \times 10^{14} \text{e/cm}^2$, respectively, the shunt leakage problem again was encountered in several cells. Cells displaying shunt leakage were omitted when computing the average powers and voltages in T3 groups. However, the short-circuit current and, thus, the minority-carrier lifetime show good recovery and stability properties in all three groups of T3 cells (Note the exception: a drop in I/I_0 from 0.94 to 0.92 between the 3rd and 6th days in group T3(1)). The only T3 group from which no cells have been lost due to shunt resistance is T3(3), the most heavily irradiated group ($3 \times 10^{15} \text{e/cm}^2$). Recovery curves for the T3(3) group are given in Figure 6. It is seen that after 3 days after irradiation, the T3(3) cells have higher power than the average of four n/p cells (D-9 to -12) irradiated to the same fluence. The initial power of the T3(3) cells, 23.1 mW, is, however, well below the n/p value of 28.1 mW.

The H4 cells, as seen in Table VII had low initial values of performance parameters. In these cells, the contact problem once again was encountered and little post-irradiation data is available at present.

TABLE VII
PHOTOVOLTAIC PERFORMANCE OF T3 AND H4 CELLS

Cell Group	(e/cm ²) ϕ	Pre-irradiation			Post-irradiation			3 Days			6 Days			11 Days		
		I_0 (mA)	P_0 (mW)	V_0 (mV)	I/I_0	P/P_0	V/V_0	I/I_0	P/P_0	V/V_0	I/I_0	P/P_0	V/V_0	I/I_0	P/P_0	V/V_0
T3(1)	1×10^{14}	61.6	23.1	584	0.74	0.72*	0.94*	0.94	0.95*	0.99*	0.92	0.93*	0.98*	0.93	0.94*	0.98*
T3(2)	$\approx 8 \times 10^{14}$	60.4	23.6	589	0.51	0.47*	0.86*	0.77	0.71**	0.92**	-	-	-	0.77	0.73**	0.93**
T3(3)	3×10^{15}	59.1	23.1	584	0.41	0.34	0.82	0.69	0.60	0.87	0.69	0.63	0.88	0.70	0.64	0.89
H4(1)	1×10^{14}	47.0	18.8	545	0.91	0.88	0.97	0.97	0.93	1.00	-	-	-	-	-	-
H4(2)	$\approx 8 \times 10^{14}$	47.5	16.1	534	0.80	0.63	0.89	-	-	-	-	-	-	-	-	-

*Only 2 cells averaged, 3rd showed shunt leakage

**Only 1 cell, others showed shunt leakage

⁷Actually H4-3539. The first two digits of the four-digit number following the lot designation on H cells have been dropped.

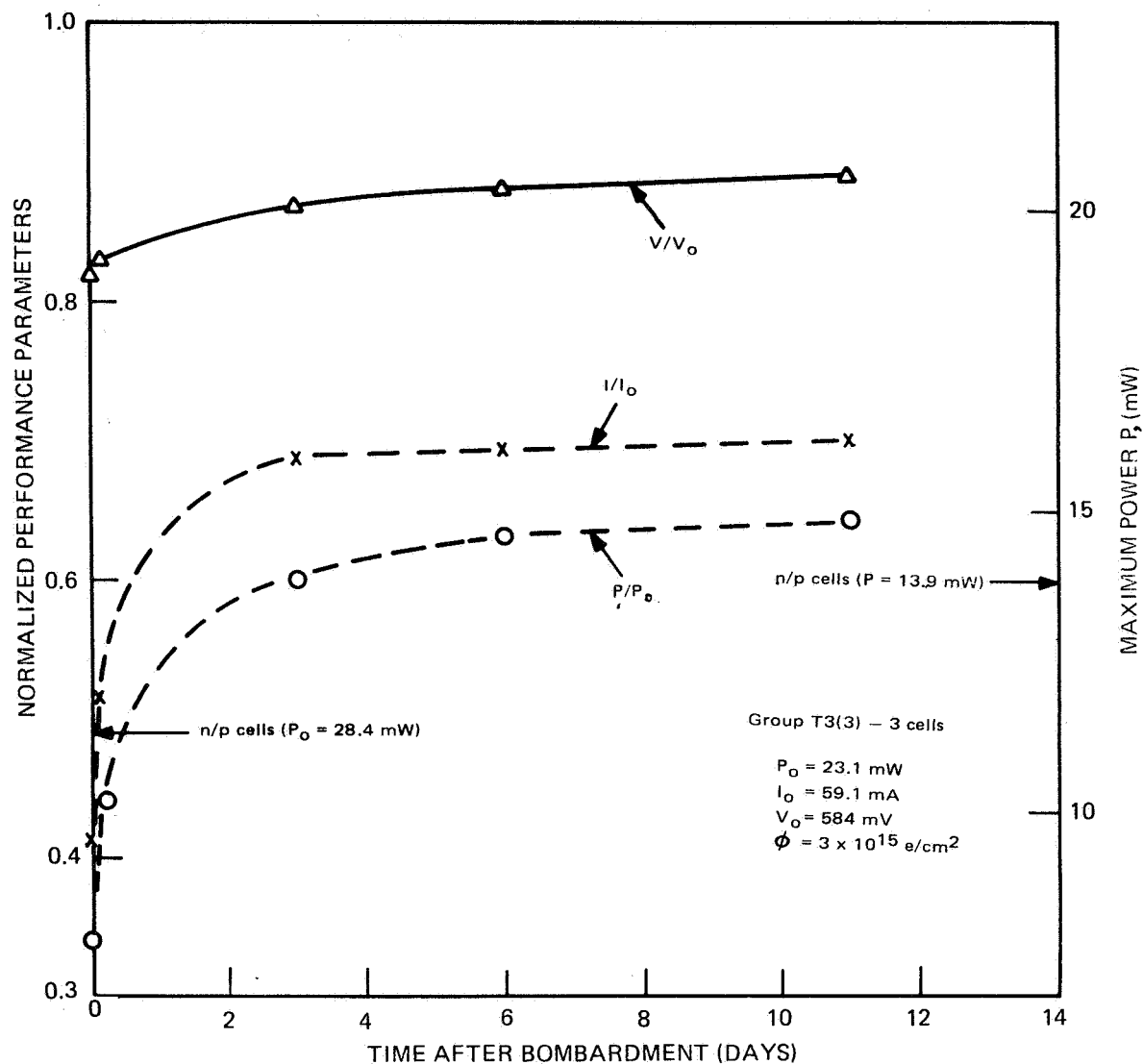


Figure 6. Cell Performance vs. Time After Irradiation to 3×10^{15} e/cm² - T3(3) Cells

E. C4 CELLS

Sixty cells from lot C4, fabricated from 100 ohm-cm Float-Zone silicon, have been tested. These cells came under five groupings or "batches". Each batch, consisting of 12 cells, underwent a given lithium diffusion schedule. For example, referring to Table VII, batch I consists of cells C4-1 to C4-12, all of which underwent a 90-minute lithium diffusion at 425°C with no subsequent distribution. Each batch was divided into four cell groups: a group of 4 cells irradiated to 1×10^{14} e/cm², a group of 3 irradiated to 5×10^{14} e/cm², a group of 3 irradiated to 3×10^{15} e/cm², and a group of 2 left unirradiated. In addition to the information noted above, Table VIII lists the approximate lithium concentrations and the initial diffusion lengths for each batch. It is seen that with the lithium diffusion cycles employed, the lithium

density in the base region near the junction decreases with increasing redistribution time. Thus, batch III has lower values of N_{LO} and dN_L/dw than batch II, which in turn, has lower values than batch I. Similarly, batch V has lower values than batch IV. It is also seen that in this lot of cells, the initial diffusion length increases with decreasing lithium concentration in agreement with the trend in most lithium cells. Unfortunately even the best batch in this regard, i.e., batch III, has a relatively low diffusion-length average of $\approx 40 \mu m$.

Table IX lists the pre-irradiation and post-irradiation photovoltaic parameters measured for these cells. The values listed are, as before, averaged over all the cells in the group unless otherwise specified. In general, cells of a given batch were similar in behavior (allowing for a ~ 10 percent spread between the highest and lowest value of I_0 in a given batch). One exception was found in cells C4-30 to -35 in batch III. These six cells displayed series resistances of approximately 1.5 ohms before irradiation. This series resistance had a severe influence on their post-irradiation behavior as will be discussed below.

In the recovery and stability studies, we will first consider the cells irradiated to $1 \times 10^{14} e/cm^2$, i.e., groups (1), (5), (9), (13) and (17). It is seen that the cells with the best initial performance, namely (9) and (17), suffer the greatest fractional degradation during irradiation, I/I_0 being 0.83 and 0.85, and P/P_0 being 0.79 and 0.82, respectively, for these groups. This was found to be the case at all three radiation fluences. Within 3 days after bombardment, all five groups have recovered to within 4 percent of the original power. As of 11 days after irradiation, only one slight trend

TABLE VIII
PROPERTIES OF C4 CELLS

Batch Group	Number of Cells	Cell Numbers	(e/cm ²)	Li Diffusion		Li Redistribution		Li Concentration		(μm)	
			ϕ	Temp(°C)	Time(Min)	Temp(°C)	Time(Min)	N _{LO} (cm ⁻³)	dN _L /dw(cm ⁻⁴)	L _o	
I	C4(1)	4	C4-1 to C4-4	1x10 ¹⁴	425	90	none	none	3x10 ¹⁵	5x10 ¹⁹	15
	(2)	3	C4-5 to C4-7	5x10 ¹⁴	425	90	none	none	3x10 ¹⁵	5x10 ¹⁹	15
	(3)	3	C4-8 to C4-10	3x10 ¹⁵	425	90	none	none	3x10 ¹⁵	5x10 ¹⁹	15
	(4)	2	C4-11 & C4-12	0	425	90	none	none	3x10 ¹⁵	5x10 ¹⁹	15
II	(5)	4	C4-13 to C4-16	1x10 ¹⁴	425	90	425	60	2x10 ¹⁵	2x10 ¹⁹	20
	(6)	3	C4-17 to C4-19	5x10 ¹⁴	425	90	425	60	2x10 ¹⁵	2x10 ¹⁹	20
	(7)	3	C4-20 to C4-22	3x10 ¹⁵	425	90	425	60	2x10 ¹⁵	2x10 ¹⁹	20
	(8)	2	C4-23 & C4-24	0	425	90	425	60	2x10 ¹⁵	2x10 ¹⁹	20
III	(9)	4	C4-25 to C4-28	1x10 ¹⁴	425	90	425	120	2x10 ¹⁴	1x10 ¹⁸	40
	(10)	3	C4-29 to C4-31	5x10 ¹⁴	425	90	425	120	2x10 ¹⁴	1x10 ¹⁸	40
	(11)	3	C4-32 to C4-34	3x10 ¹⁵	425	90	425	120	2x10 ¹⁴	1x10 ¹⁸	40
	(12)	2	C4-35 & C4-36	0	425	90	425	120	2x10 ¹⁴	1x10 ¹⁸	40
IV	(13)	4	C4-37 to C4-40	1x10 ¹⁴	450	40	none	none	2x10 ¹⁵	2x10 ¹⁹	15
	(14)	3	C4-41 to C4-43	5x10 ¹⁴	450	40	none	none	2x10 ¹⁵	2x10 ¹⁹	15
	(15)	3	C4-44 to C4-46	3x10 ¹⁵	450	40	none	none	2x10 ¹⁵	2x10 ¹⁹	15
	(16)	2	C4-47 & C4-48	0	450	40	none	none	2x10 ¹⁵	2x10 ¹⁹	15
V	(17)	4	C4-49 to C4-52	1x10 ¹⁴	450	40	450	80	3x10 ¹⁴	1x10 ¹⁸	30
	(18)	3	C4-53 to C4-55	5x10 ¹⁴	450	40	450	80	3x10 ¹⁴	1x10 ¹⁸	30
	(19)	3	C4-56 to C4-58	3x10 ¹⁵	450	40	450	80	3x10 ¹⁴	1x10 ¹⁸	30
	(20)	2	C4-59 & C4-60	0	450	40	450	80	3x10 ¹⁴	1x10 ¹⁸	30

TABLE IX
PHOTOVOLTAIC PERFORMANCE OF C4 CELLS

Group	(e/cm ²) β	Pre-irradiation		Post-irradiation		150 Min		3 Days		6 Days		11 Days	
		I ₀ (mA)	P ₀ (mW)	V ₀ (mV)	I/I ₀	P/P ₀	V/V ₀	I/I ₀	P/P ₀	V/V ₀	I/I ₀	P/P ₀	V/V ₀
Batch I													
C4(1)	1x10 ¹⁴	39.1	13.8	537	0.92	0.90	0.98	-	0.97	0.97	0.99	0.97*	1.00*
(2)	5x10 ¹⁴	40.2	15.8	539	0.83	0.77	0.94	-	0.96	0.87	0.98	-	-
(3)	3x10 ¹⁵	39.1	15.3	532	0.71	0.59	0.88	0.84	0.71	0.89	0.97	0.84*	0.91*
(4)	0	40.3	15.7	539	-	-	-	-	-	-	-	-	-
Batch II													
(5)	1x10 ¹⁴	44.3	17.7	534	0.90	0.86	0.96	-	0.99	0.98	0.99	0.98*	0.99*
(6)	5x10 ¹⁴	45.4	17.5	531	0.77	0.69	0.91	-	0.99	0.95	0.98	0.99*	0.96*
(7)	3x10 ¹⁵	44.9	17.7	531	0.59	0.46	0.84	0.74	0.51	0.84	0.94	0.72	0.87
(8)	0	46.2	17.7	532	-	-	-	-	-	-	-	-	-
Batch III													
(9)	1x10 ¹⁴	54.5	21.1	532	0.83	0.79	0.95	-	0.96	0.97	0.99	0.98	0.98
(10)	5x10 ¹⁴	55.2	20.3	538	0.69	0.60	0.86	-	0.95	0.83	0.94	0.99	0.86
** (11)	3x10 ¹⁵	54.7	19.1	538	0.59	0.38	0.77	0.61	0.38	0.77	0.73	0.34	0.77
(12)	0	55.3	19.9	535	-	-	-	-	-	-	-	-	-
Batch IV													
(13)	1x10 ¹⁴	38.8	15.0	525	0.95	0.91	0.98	-	0.98	0.96	0.99	0.99*	0.99*
(14)	5x10 ¹⁴	38.9	15.3	527	0.89	0.82	0.95	-	0.98	0.95	0.99	0.97*	0.93*
(15)	3x10 ¹⁵	38.7	15.1	517	0.74	0.63	0.89	1.84	0.72	0.89	0.97	0.86	0.94
(16)	0	39.0	14.3	526	-	-	-	-	-	-	-	-	-
Batch V													
(17)	1x10 ¹⁴	51.7	19.6	528	0.85	0.82	0.95	-	1.00	0.99	0.99	1.00	0.99
(18)	5x10 ¹⁴	53.1	20.8	535	0.70	0.61	0.88	-	0.97	0.90	0.95	0.99	0.91
(19)	3x10 ¹⁵	50.5	20.0	530	0.60	0.43	0.81	0.62	0.44	0.81	0.85	0.57	0.82
(20)	0	53.4	21.4	532	-	-	-	-	-	-	-	-	-

Only one cell measured
**High series resistance

*Only one cell measured

**High series resistance

toward redegradation is observed. This occurs in group C4(1) where all of the cells display a slight (≈ 1 percent) drop in open-circuit voltage, and consequently power, relative to the 3-day reading. It is too early to ascertain whether this drop is significant.

The cells in groups (2), (6), (10), (14), and (18) were irradiated to $5 \times 10^{14} \text{e/cm}^2$. These cells have partially recovered in the 11 days since irradiation with indications of redegradation present only in cells C4-30 and -31 of group (10), two of the cells with high initial series resistance. The redegradation experienced by these two cells is in the form of a small increase in series resistance from ≈ 1.4 ohms immediately after irradiation to ≈ 1.7 ohms six days after irradiation. During the time in which this series-resistance increase occurred, short-circuit current recovery was also taking place so that the net result was a slight increase in the output of these two cells. The other cell of group (10), C4-29, had a lower initial series resistance, 0.7 ohm. This cell also showed a slight post-irradiation resistance increase to 0.85 ohm which occurred between the first and sixth day after irradiation.

The cells in groups (3), (7), (11), (15), and (19) were irradiated to $3 \times 10^{15} \text{e/cm}^2$. The recovery curves for these five groups are given in Figures 7 to 11. No degradation has yet been observed in cells of groups (3), (7), (15), and (19). Group C4(11), shown in Figure 9, suffer continuing degradation in power output after irradiation. The cells of C4(11) are C4-32 to -34 which initially had high-series resistances of ≈ 1.5 ohms. Immediately after irradiation, the series resistance in these cells was ~ 2.7 ohms, and six days after irradiation was 4.5 ohms. Thus, the degradation in power was (probably entirely) due to the increase in series resistance. The pre-irradiation photovoltaic characteristics of C4-32 are given in Figure 12 for illumination by 140 mW/cm^2 tungsten and for $\sim 70 \text{ mW/cm}^2$ illumination. The series resistance was obtained (Reference 7) from the curves by measuring the voltage at a point offset an equal amount, in this case 6.5 mA, from the short-circuit current point on each curve. By taking the difference in this voltage between the two curves (0.038 V) and dividing by the difference in short-circuit current (25.3 mA) the resistance is found to be ≈ 1.5 ohms. Post-irradiation curves for C4-32 taken at 140 mW/cm^2 are shown in Figure 13. Curves are given for 20 minutes, 150 minutes, 3 days, and 11 days after irradiation. These curves clearly show the effect of increasing resistance on the curve shape and power output. The series resistance was directly measured in the 20-minute, 150-minute, and 3-day curves by the method of Figure 12. By the sixth day after irradiation the series resistance had become sufficient to significantly effect the short-circuit current. This is shown in the 11-day curve where a significant negative slope is seen at the current intercept. In order to get accurate measurements of light-generated current and series resistance under these conditions, it would be necessary to drive the terminal voltage sufficiently negative to reduce the p/n junction bias to zero.

The cells in group C4(7), C4-20 to -22, all developed a ≈ 300 ohm shunt leakage immediately after irradiation. The shunt resistance has since remained at this ≈ 300 ohm value. The three cells from group C4(19), C4-56 to -58, developed series resistances of ≈ 1.5 ohms and shunt leakages of ≈ 150 ohms during irradiation. These

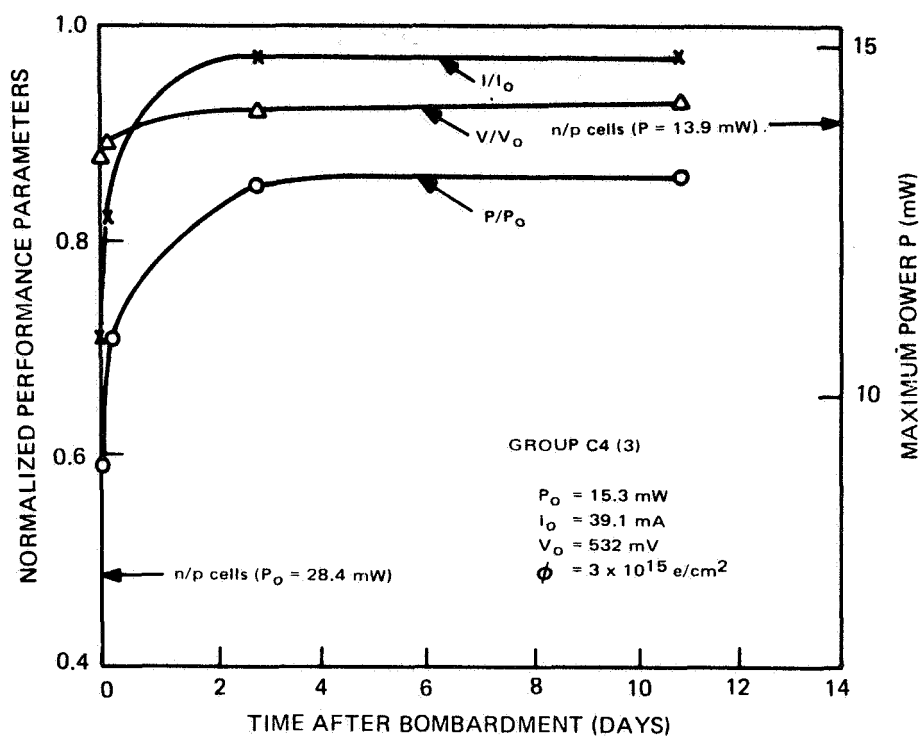


Figure 7. Cell Performance vs. Time After Irradiation to $3 \times 10^{15} \text{ e/cm}^2$ - C1(1) Cells

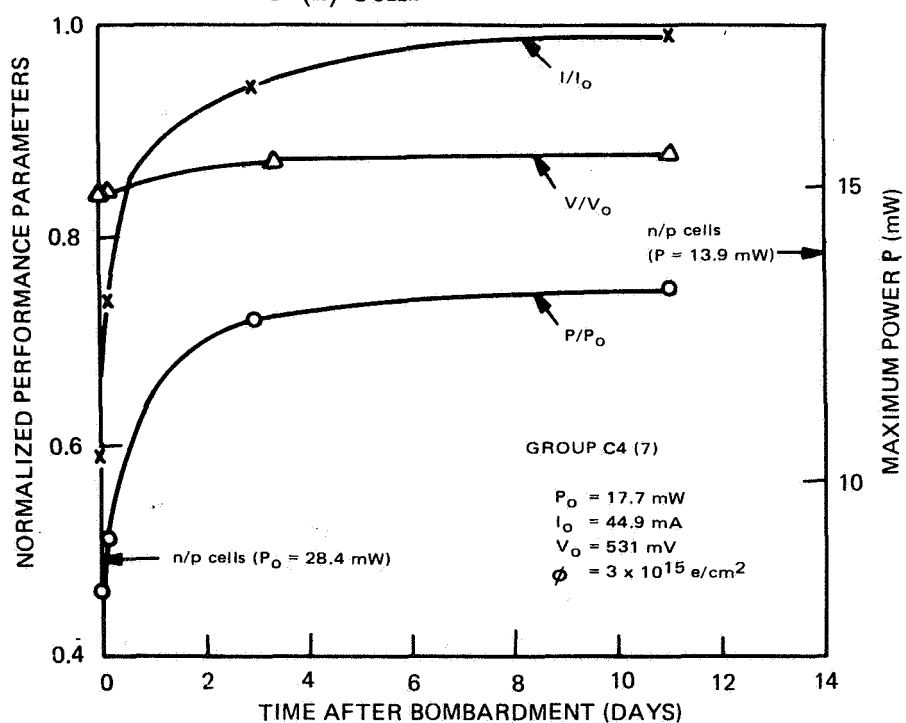


Figure 8. Cell Performance vs. Time After Irradiation to $3 \times 10^{15} \text{ e/cm}^2$ - C4(7) Cells

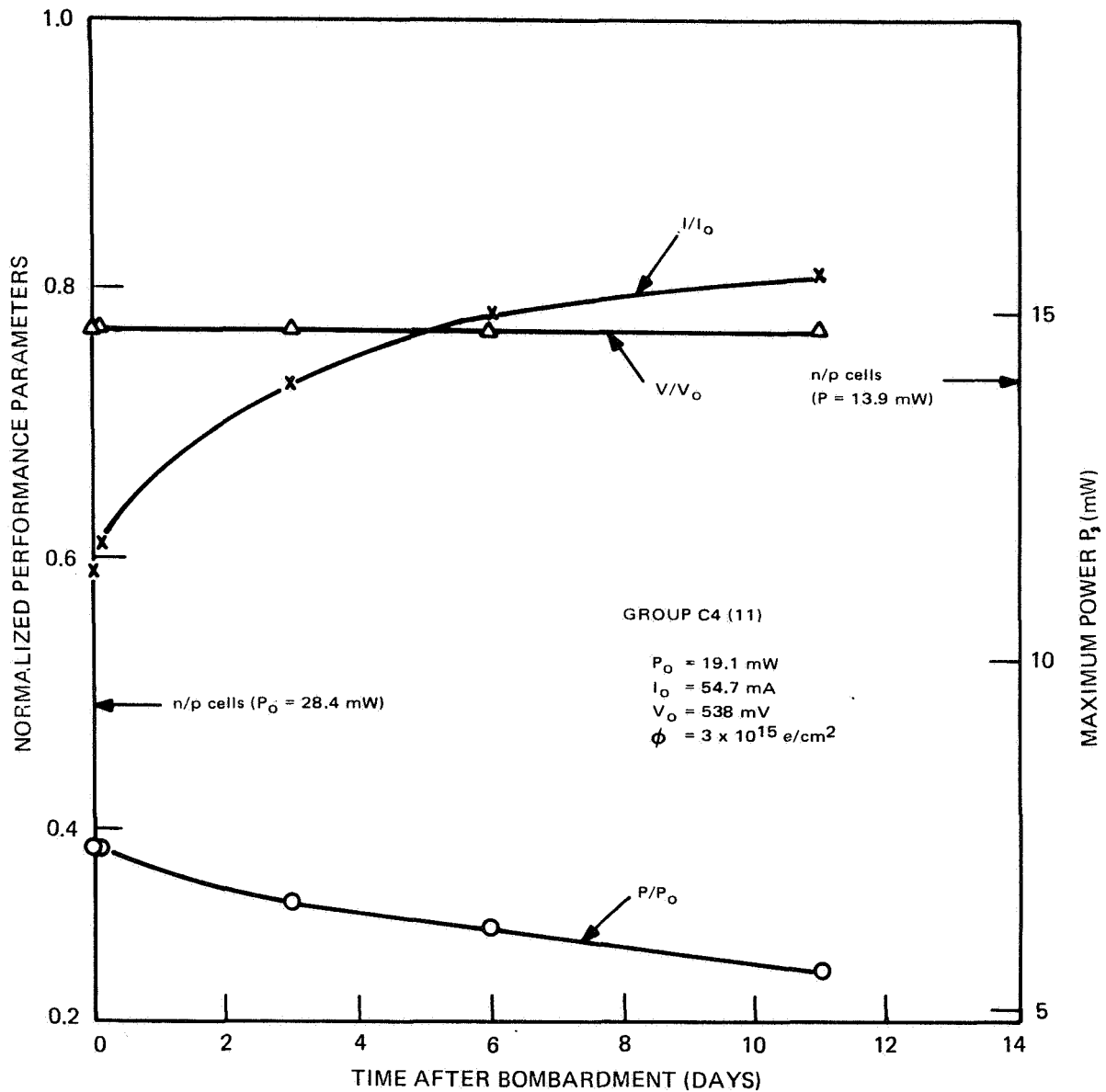


Figure 9. Cell Performance vs. Time After Irradiation to 3×10^{15} e/cm² - C4(11) Cells

resistances have also remained constant since immediately after irradiation. Groups C4(3) and C4(15), which are the two groups with poorest initial performance, have displayed no post-irradiation irregularities. A very interesting element in the post-irradiation behavior of the cells irradiated to 3×10^{15} e/cm² is the almost total recovery of the short-circuit current. This is readily seen in Table IX and in Figures 7 to 11. Where series and shunt resistances are absent, almost all of the loss in performance of the recovered cell with respect to the pre-irradiation performance is due to a loss in open-circuit voltage. This is quite the opposite of the situation in n/p cells (Reference 12), and in lithium cells immediately after irradiation where the short-circuit current loss is the larger factor in cell degradation.

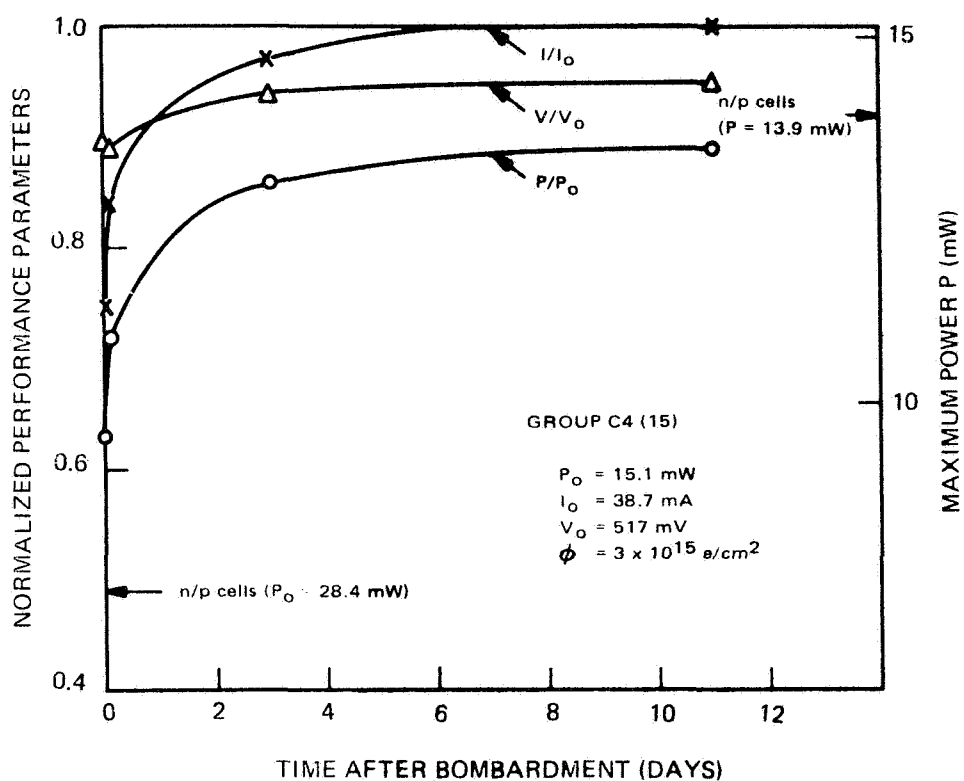


Figure 10. Cell Performance vs. Time After Irradiation to 3×10^{15} e/cm² - C4 (15) Cells

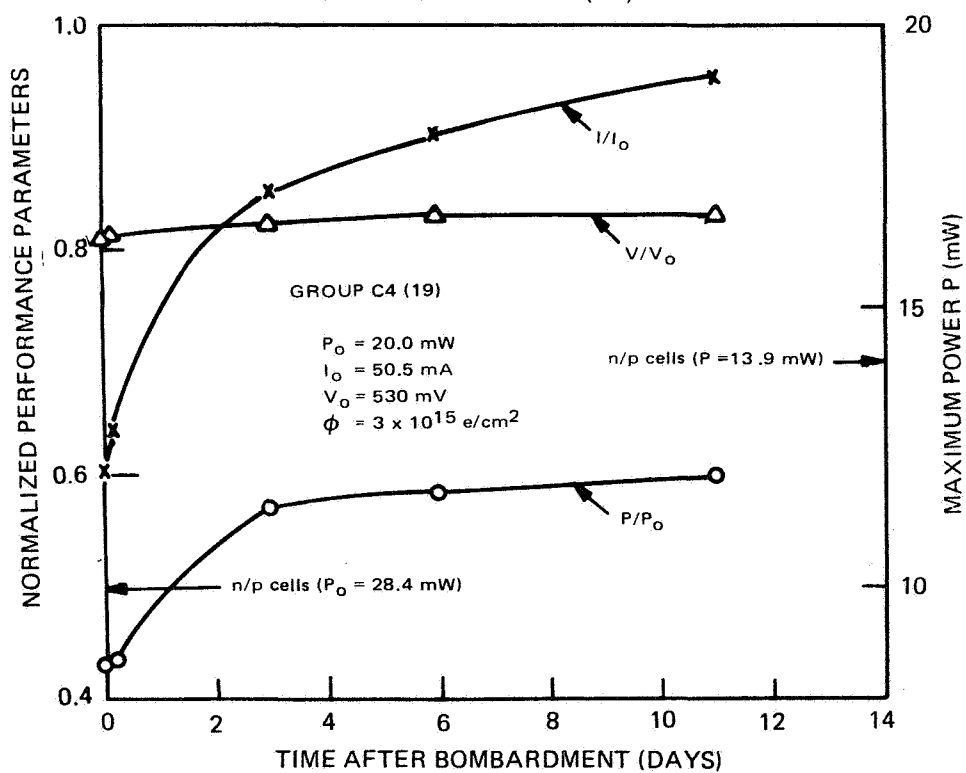


Figure 11. Cell Performance vs. Time After Irradiation to 3×10^{15} e/cm² - C4(19) Cells

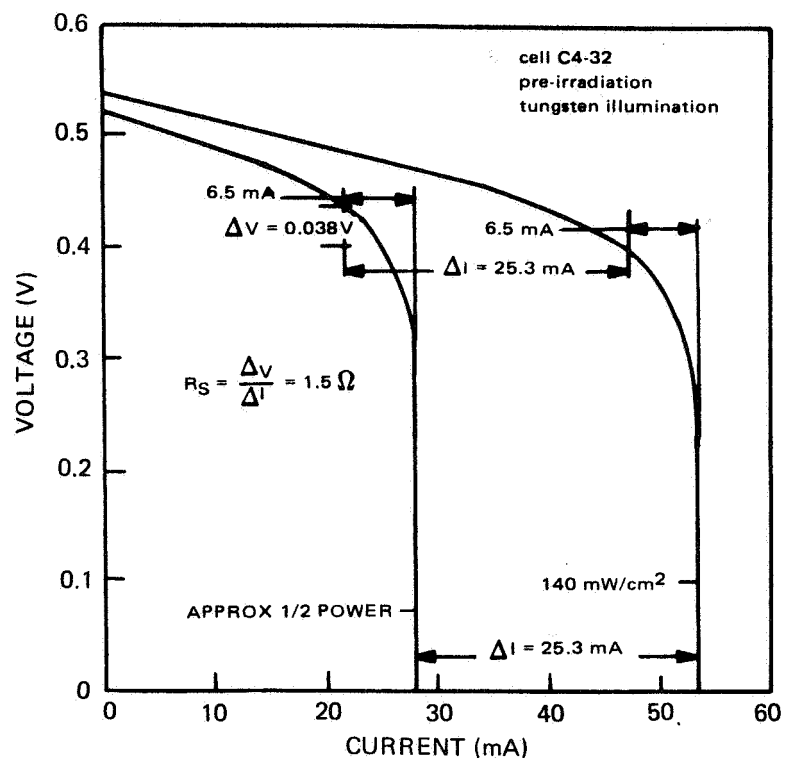


Figure 12. Pre-irradiation I-V Curves for Cell C4-32 at Two Light Levels

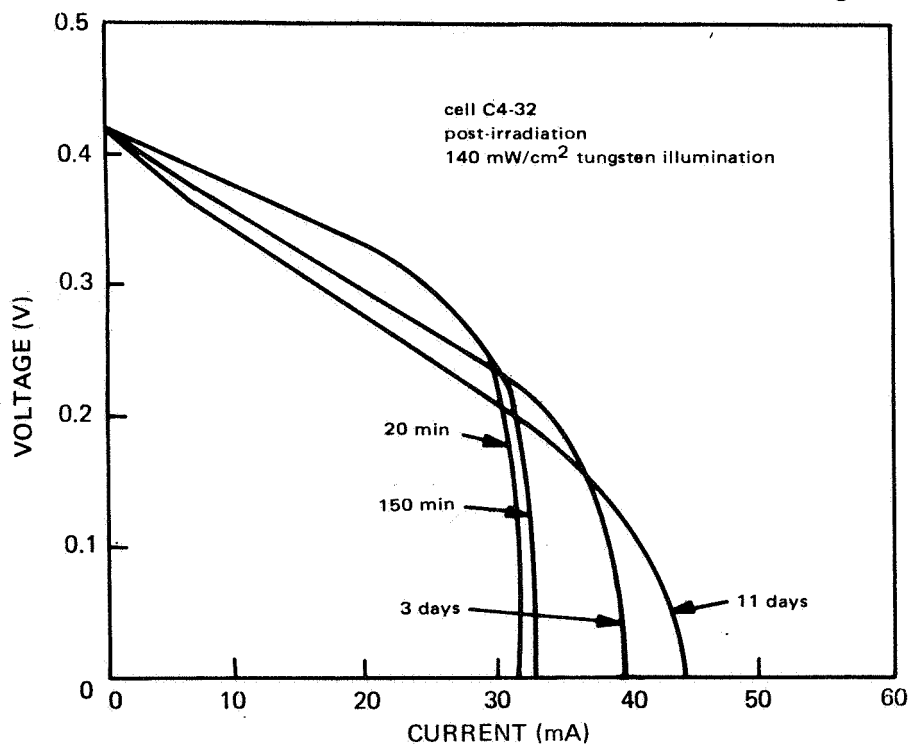


Figure 13. Post-irradiation I-V Curves for Cell C4-32 Taken With 140 mW/cm² Tungsten Illumination

Attempts were made to relate this behavior to physical parameters through investigation of the equations for short-circuit current and open-circuit voltage (References 8, 13)

$$J = 15.5 \log_{10} \left[(D_p \tau_p)^{1/2} \right] \quad (1)$$

and

$$V = 0.0575 \log_{10} J_L \left[\frac{0.062 \exp(39E_g)}{\rho_n \mu_n D_p} (D_p \tau_p)^{1/2} \right] \quad (2)$$

where

J is short-circuit current density,

D_p is the minority-carrier diffusion constant in the n type base,

τ_p is the minority-carrier lifetime,

E_g is the silicon band gap,

ρ_n is the resistivity of the base region, and

μ_n is the majority-carrier mobility in the base.

The equations indicate that the observed behavior of full short-circuit current recovery and permanent open-circuit voltage degradation would occur only if the product of $\rho_n \mu_n D_p$ significantly increased. Clearly, neither μ_n nor D_p increase: previous results (see Appendix I of Reference 4b) show that μ_n remains constant at room temperature. Thus, an effective increase in ρ_n is required for the observed changes. Such an effective increase in ρ_n is reasonable in view of the previously observed (Reference 4) weakness of the p/n junction in lithium cells. It is thus concluded that the apparently permanent degradation in open-circuit voltage in these cells is due to changes occurring in the junction itself rather than to any effects in the bulk of the base region in the cell.

SECTION III

CONCLUSIONS AND FUTURE PLANS

A. CONCLUSIONS

The work in the present reporting period, consisting purely of cell evaluations, has produced some surprising examples of non-recovery and unexpectedly rapid recoveries in JPL-furnished cells. There is evidence that not all important processing problems for lithium cells have yet been solved. It is also clear that there is at least one type of cell redegradation possible which is totally unrelated to minority-carrier lifetime redegradation.

The results of the recovery and stability tests on a large number of JPL-furnished p/n lithium-containing solar cells show that Quartz-Crucible cells were free from redegradation for the first 69 days after irradiation to a fluence of $1 \times 10^{14} \text{e/cm}^2$. One group of cells (lot C2), however, showed no significant recovery over this period of time. By contrast, another group (lot T2) displayed recovery times, i.e., ≈ 10 days, which were unusually short for Quartz-Crucible cells.

Cells fabricated from Quartz-Crucible silicon, Lopex silicon, and Float-Zone silicon were more recently irradiated to higher fluences (5×10^{14} and $3 \times 10^{15} \text{e/cm}^2$). In the first eleven days since irradiation, all of these cells except those from lot C2 recovered, to varying degrees, in short-circuit current. No cells have yet shown any significant redegradation in short-circuit current. However, in three cells of lot C4 (Float-Zone) irradiated to a fluence of $3 \times 10^{15} \text{e/cm}^2$, rapid degradation in power was observed to continue after irradiation had ceased. This was attributed to an increase in series resistance, probably contact resistance, after irradiation. This resistance was observed to increase with time after irradiation and, hence, probably has relevance to the redegradation problem. Several cells from lot T2 (Quartz-Crucible) displayed unduly low shunt resistances both before and after irradiation. Several cells from both Quartz-Crucible and Float-Zone lots developed shunt resistances of ≥ 100 ohms which appeared in the measurements taken immediately after irradiation. In all five groups of the C4 group, which were irradiated to $3 \times 10^{15} \text{e/cm}^2$, the relative damage to open-circuit voltage degradation remaining after 11 days recovery time was greater than the remaining damage to short-circuit current. These results, together with stability results reported in the previous reporting

period, lead to the strong suspicion that weakness in the junction properties and contacts are more common causes for problems in lithium cells than is redegradation of minority-carrier lifetime. The accumulated experience on lithium cells however, indicates that several redegradation mechanisms, including lifetime reduction, may be simultaneously operative, depending on the initial cell properties and the level of radiation. In the present tests it is too soon to see any relationship between cell stability properties and previous work (Reference 4b) on carrier removal and mobility in bulk silicon.

Measurements on five batches of C4 cells which had undergone different lithium diffusion and redistribution schedules showed that the batches undergoing longer redistribution cycles had lower lithium densities near the junction and higher initial minority-carrier diffusion lengths and initial photovoltaic outputs.

B. FUTURE PLANS

Stability tests on both irradiated and unirradiated JPL-furnished cells will be continued. Attempts will be made to relate changes in photovoltaic response to cell physical characteristics through light and dark I-V measurements and capacitance measurements. Correlations between this work and previous work on solar cells and bulk silicon will be sought.

LIST OF REFERENCES

1. J.J. Wysocki, P. Rappaport, E. Davison, R. Hand, and J. J. Loferski, Appl. Phys. Letters 9, 44 (1966).
2. G.J. Brucker, T. Faith, and A.G. Holmes-Siedle, Final Report on Contract No. NAS5-10239, prepared by RCA and issued March 8, 1968.
3. T. R. Waite, Phys. Rev. 107, 463 (1957).
- 4(a). T.J. Faith, G.J. Brucker, A.G. Holmes-Siedle and J. Wysocki "Long Term Stability of Lithium-Doped Solar Cells Irradiated with Protons, Electrons, or Neutrons," Presented at Seventh Photovoltaic Spec. Conf., Jet Propulsion Laboratory, Pasadena, Calif., Nov. 20, 1968.
- 4(b). G. J. Brucker, T. J. Faith and A. G. Holmes-Siedle, Second Quarterly Report on Contract No. 952249, prepared by RCA and issued November 15, 1968.
5. H. J. Stein and F. L. Vook, Phys. Rev. 163, 790 (1967); "Radiation Effects in Semiconductors," Edited by F. L. Vook. (Plenum Publishing Corporation, New York, 1968) p. 115.
6. H. Gummel and F. Smits, Bell Syst. Tech. Journ. 43, 1103 (1964).
7. M. Wolf and H. Rauschenbach, Adv. Energy Conversion 3, 455 (1963).
8. G. Brucker, T. Faith, and A. Holmes-Siedle, "Injection-Level Effects in Irradiated, Lithium-Containing Solar Cells," presented at Seventh Photovoltaic Spec. Conf., Jet Propulsion Laboratory, Pasadena, Calif., Nov. 20, 1968.
9. P. Iles, "Effect of Lithium on Solar Cell Properties," presented at Seventh Photovoltaic Spec. Conf., Jet Propulsion Laboratory, Pasadena, Calif., Nov. 20, 1968.
10. Properties of Solar Cells C4-1 to C4-60, private communication from P. Berman.
11. C. Sah and V. Reddi, IEEE Trans. on Electron Devices ED 11, 345, 1964.
12. W. R. Cherry and R. L. Statler, GSFC Report X-716-68-204 (April 1968).
13. M. B. Prince, J. Appl. Phys., 26, 534, (1955).

